

ARTICLES

Evidence of Rotational Isomerism in 1-Butyl-3-methylimidazolium Halides: A Combined High-Pressure Infrared and Raman Spectroscopic Study[†]Hai-Chou Chang,^{*,‡} Jyh-Chiang Jiang,[§] Jong-Chang Su,[‡] Chao-Yen Chang,[‡] and Sheng Hsien Lin^{||,⊥}

Department of Chemistry, National Dong Hwa University, Shoufeng, Hualien 974, Taiwan, Department of Chemical Engineering, National Taiwan University of Science and Technology, Taipei 106, Taiwan, Institute of Atomic and Molecular Sciences, Academia Sinica, P.O. Box 23-166, Taipei 106, Taiwan, and Department of Chemistry, National Taiwan University, Taipei 106, Taiwan

Received: February 7, 2007; In Final Form: March 20, 2007

High-pressure methods were applied to investigate the rotational isomerism and the hydrogen-bonding structures of 1-butyl-3-methylimidazolium bromide and 1-butyl-3-methylimidazolium chloride, respectively. Conformation changes of the butyl chain were observed above a pressure of 0.3 GPa. Under ambient pressure, Raman spectra indicate that the more thermodynamically stable butyl structure of the cations is the gauche–anti (GA) and all-anti forms for 1-butyl-3-methylimidazolium bromide and 1-butyl-3-methylimidazolium chloride, respectively. Nevertheless, the high-pressure phases arise from the perturbed GA conformer. The imidazolium C–H bands of 1-butyl-3-methylimidazolium chloride display anomalous nonmonotonic pressure-induced frequency shifts. This discontinuity in the frequency shift is related to the modification of the imidazolium C–H...Cl[−] contacts upon compression. The alkyl C–H...Cl[−] interactions are suggested to be a compensatory mechanism to provide additional stability. Density-functional-theory-calculated results also support the high-pressure results that the methyl and butyl C–H groups are suitable proton donor sites for the GA conformer.

Introduction

In recent years ionic liquids have been used as novel solvent systems for green chemistry and liquid electrolytes.^{1–4} The key property is that the vapor pressure of ionic liquids is negligibly small, thus making them green solvents by reducing environmental levels of volatile organic carbons. Ionic liquids have a melting temperature around room temperature and are built up by a bulky, asymmetric organic cation, such as 1-alkyl-3-methylimidazolium,^{1–6} to prevent ions from packing easily. The liquid structure of ionic liquids results from a competition between screening and packing. This means a balance between long-range electrostatic forces and geometric factors. Ionic liquids are often denoted as designer solvents because of the versatility of their properties, which is a consequence of the ease of interchanging anions and cations that leads to a huge number of combinations.^{1,2} Although ionic liquids have attracted much attention from scientists because of their useful characteristics, some fundamental questions still remain to be answered regarding the nature of the liquid state. Although the results of crystal structures are highly informative on the relative geometry changes, crystallography does not provide direct information

on the local structure in the liquid phase. It is not clear whether the solid-structure is equivalent to that found in liquid or not.

Evidence of crystal polymorphism in 1-butyl-3-methylimidazolium-based ionic liquids has been obtained.^{7–10} The morphological feature of 1-butyl-3-methylimidazolium-based ionic liquids has been proposed as a plausible rationalization of their low melting point.^{7,8} 1-Butyl-3-methylimidazolium chloride forms two different crystal polymorphs at room temperature: monoclinic and orthorhombic. The conformation feature of the cation that differentiates these two types of crystals is the torsion angle around C⁷–C⁸ in the butyl chain. In the monoclinic form, the conformation of the butyl chain is all anti, and in the orthorhombic form the chain is gauche around C⁷–C⁸. In a convenient notation, these conformers are referred to here as the AA (all-anti) and the GA (gauche–anti) forms. 1-Butyl-3-methylimidazolium chloride in the AA form seems to be a more thermodynamically stable form at ambient pressure.^{7,8} Nevertheless, a significant change in conformational preference occurs upon switching the counteranion from Cl[−] to Br[−]. The only stable alkyl structure of 1-butyl-3-methylimidazolium bromide observed under ambient pressure is the GA form.⁸ It is important to characterize the conformational equilibria present in these systems because the alkyl groups are among the most fundamental structural units in chemistry.

Previous studies of the structure of alkyl side chains have included the use of X-ray crystallography and vibrational spectroscopy at ambient pressure.^{7–14} The Raman spectra of AA and GA conformers differ considerably when recorded at

[†] Part of the “Sheng Hsien Lin Festschrift”.

^{*} To whom correspondence should be addressed. E-mail: hcchang@mail.ndhu.edu.tw; fax: +886-3-8633570; phone: +886-3-8633585.

[‡] National Dong Hwa University.

[§] National Taiwan University of Science and Technology.

^{||} Institute of Atomic and Molecular Sciences.

[⊥] National Taiwan University.

room temperature and ambient pressure.^{11–13} The presence of two crystalline polymorphs suggests that the potential energy surface for 1-butyl-3-methylimidazolium chloride contains two (or more) local conformational energy minima. Inhibition of crystallization through the provision of a large number of similarly stabilized solid-state structures may lead to plasticity and low melting points. The tendency to crystallize at low (high) enough temperature (pressure) might be a potential limitation for some ionic liquids, especially when one wishes to use them at temperatures below (above) ambient conditions. For this reason, a detailed understanding of the phase diagram of ionic liquids is of high importance to further extend the range of applications for these important green materials.

Recent studies have been performed to elucidate the role of weak hydrogen-bonds, such as C–H...O and C–H...X, in the structure of ionic liquids.^{3,4,15–17} There has been a longstanding discussion as to the nature of weak hydrogen-bonding, but experimental evidence of such interaction is notoriously difficult to obtain. One of the intriguing aspects of weak hydrogen-bonds is that the C–H stretching band undergoes a blue-shift when the C–H groups form weak hydrogen-bonds. This behavior is opposite to that of the classical hydrogen-bond, and its underlying mechanism is not well understood. Two schools of thought have emerged to try to explain its physical basis.^{18–20} Hobza et al.¹⁸ suggested that the strengthened C–H bond originates from a new mechanism, called anti-hydrogen-bonding. Scheiner¹⁹ and Dannenberg,²⁰ however, view conventional and weak hydrogen-bonds to be very similar in nature and believe that both types of hydrogen-bonds result from a combination of electrostatic, polarization, charge-transfer, dispersion, and exchange/steric repulsion forces between the proton donor and the acceptor. One of the underlying reasons for this controversy is the weakness of weak hydrogen-bonds. Therefore, methods that enhance weak hydrogen-bonding are crucial to provide scientists with a clear and unified view of this important phenomenon. Studies have shown the potential significance that pressure has on controlling the strength of weak hydrogen-bonds.^{21–24} To get direct information about C–H...X interactions in ionic liquids, we probe 1-butyl-3-methylimidazolium halides (Cl[−] and Br[−]) with pressure in this study.

Generally, vibrational studies were performed at ambient pressure and mostly at room temperature, although interest in pressure as an experimental variable has been growing in physicochemical studies. The use of pressure as a variable allows one to change, in a controlled way, the intermolecular interactions without encountering the major perturbations produced by changes in temperature and chemical composition. Under high-pressure conditions, the relative weights of the strong intramolecular interactions responsible for molecular bonding and of the weaker intermolecular forces defining the aggregation states are altered, and the repulsive side of the intermolecular potential is explored. This is particularly useful because little is known about the relative importance of the hydrophilic vs hydrophobic part of molecules in the collapse and aggregation processes. In this study, we use variable pressure as a window into the structural organization of the N-alkyl moiety in ionic liquids.

Experimental Section

Samples were prepared using 1-butyl-3-methylimidazolium chloride (>90%) and 1-butyl-3-methylimidazolium bromide (>97%) supplied by Fluka. A diamond anvil cell (DAC) of the Merrill–Bassett design, having a diamond culet size of 0.6 mm, was used for generating pressures up to ca. 2 GPa. Two type-

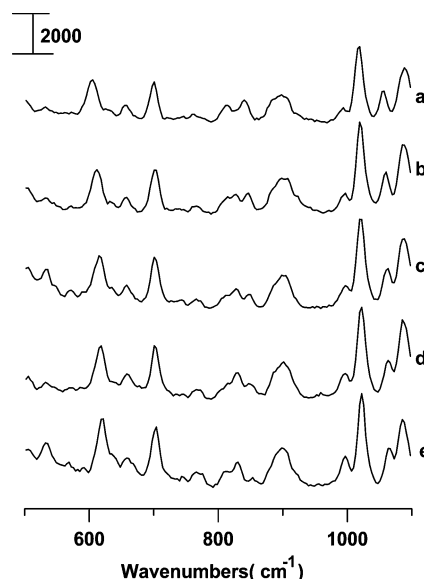


Figure 1. Pressure-dependence of the Raman spectra of pure 1-butyl-3-methylimidazolium bromide under the following pressures: (a) ambient, (b) 0.3, (c) 0.9, (d) 1.5, and (e) 1.9 GPa. The Raman intensity (counts) is labeled on the top left corner.

Ila diamonds were used for mid-infrared (IR) measurements. The sample was contained in a 0.3 mm diameter hole in a 0.25 mm thick inconel gasket mounted on the diamond anvil cell. To reduce the absorbance of the samples, CaF₂ crystals (prepared from a CaF₂ optical window) were placed into the holes and were compressed firmly prior to inserting the samples. A droplet of a sample filled the empty space of the entire hole of the gasket in the DAC, which was subsequently sealed when the opposed anvils were pushed toward one another. Infrared spectra of the samples were measured on a Perkin-Elmer Fourier transform spectrophotometer (model Spectrum RX1) equipped with a LITA (lithium tantalite) mid-IR detector. The IR beam was condensed through a 5× beam condenser onto the sample in the diamond anvil cell. Typically, we chose a resolution of 4 cm^{−1} (data point resolution of 2 cm^{−1}). For each spectrum, typically, 1000 scans were compiled. To remove the absorption of the diamond anvils, the absorption spectra of the DACs were measured first and were subtracted from those of the samples. Pressure calibration follows Wong's method.^{25,26} The pressure-dependence on the screw moving distances was measured.

The Raman spectra were measured using a 100 mW diode pumped solid-state (DPSS) laser ($\lambda = 532$ nm) and a microscope-based Raman spectrometer having a 300 mm spectrograph (Acton SP308) and equipped with a 1200 gr/mm holographic grating and a side window photon counting detector system. Two type-Ia diamonds were used for Raman measurements. We chose a 100 μ m slit width, corresponding to a resolution of ca. 5 cm^{−1}. CaF₂ crystals were not used for high-pressure Raman measurements.

Results and Discussion

Figure 1 displays Raman spectra of 1-butyl-3-methylimidazolium bromide in the crystalline form obtained under ambient pressure (curve a) and at 0.3 (curve b), 0.9 (curve c), 1.5 (curve d), and 1.9 GPa (curve e). Raman characteristic bands appear at 604 and 700 cm^{−1}, as shown in Figure 1a. It is known that the structure of the 1-butyl-3-methylimidazolium cation in 1-butyl-3-methylimidazolium bromide is essentially the same as that in 1-butyl-3-methylimidazolium chloride in the GA form, and the observed characteristic bands of the GA conformer at

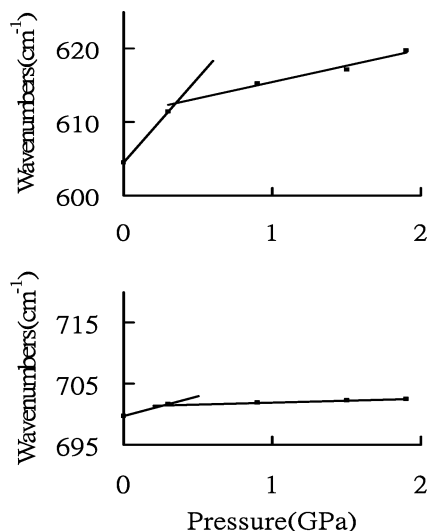


Figure 2. Pressure-dependence of the maximum positions of the characteristic bands of 1-butyl-3-methylimidazolium bromide at ca. 600 and 700 cm^{-1} .

604 and 700 cm^{-1} in Figure 1a are in agreement with the literature.^{8,12} As the sample was compressed, that is, increasing the pressure from ambient (Figure 1a) to 0.3 GPa (Figure 1b), we observed that the characteristic bands were blue-shifted to 611 and 702 cm^{-1} , respectively. We note that the 604 cm^{-1} band is more pressure-sensitive than the band at ca. 700 cm^{-1} . As the sample was further compressed, that is, increasing the pressure from 0.3 GPa (Figure 1b) to 1.9 GPa (Figure 1e), we observed a monotonic blue-shift in frequency for the characteristic bands at ca. 604 and 700 cm^{-1} , respectively. To illustrate the frequency shift, the pressure-dependence of the maximum positions of the characteristic bands of the GA conformer was plotted in Figure 2. Slopes ($\text{d}\nu/\text{d}P$) of 23 and 6 $\text{cm}^{-1}/\text{GPa}$ were obtained for the bands at ca. 604 and ca. 700 cm^{-1} , respectively, below a pressure of 0.3 GPa. Nevertheless, the pressure-induced frequency shifts of the characteristic bands are relatively small under pressures above 0.3 GPa. Slopes ($\text{d}\nu/\text{d}P$) of 4 and 1 $\text{cm}^{-1}/\text{GPa}$ were obtained for the bands at ca. 604 and ca. 700 cm^{-1} , respectively, above a pressure of 0.3 GPa. This may indicate a pressure-induced structural transformation above a pressure of 0.3 GPa. The monotonic blue-shift in frequency for the characteristic bands ($P > 0.3$ GPa) suggests that the new high-pressure phase seems to be thermodynamically stable up to pressures of 1.9 GPa. The spectral profiles in Figure 1 did not have dramatic changes as the pressure was elevated to >0.3 GPa. Therefore, we suggest that the new high-pressure phase of 1-butyl-3-methylimidazolium bromide arises from the perturbed GA conformer, that is, distorted Crystal 2.^{7,8}

Figure 3 displays Raman spectra of 1-butyl-3-methylimidazolium chloride in crystalline form obtained under ambient pressure (curve a) and at 0.3 (curve b), 0.9 (curve c), 1.5 (curve d), and 1.9 GPa (curve e). The two characteristic bands of the AA form (Crystal 1) appear at 626 and 733 cm^{-1} , as revealed in Figure 3a. The results are in agreement with the fact that Crystal 1 is a more thermodynamically stable form under the condition of ambient pressure. The spectral profiles underwent dramatic changes as the pressure was elevated to 0.3 GPa in Figure 3b. The observation of the characteristic bands at 613 and 700 cm^{-1} in Figure 3b indicates that a high-pressure phase of 1-butyl-3-methylimidazolium chloride is formed. The similarity between Figures 1b and 3b suggested that Figure 3b originates from a Crystal 2-like structure, that is, the distorted GA form. At a pressure of 0.9 GPa (Figure 3c), the spectral

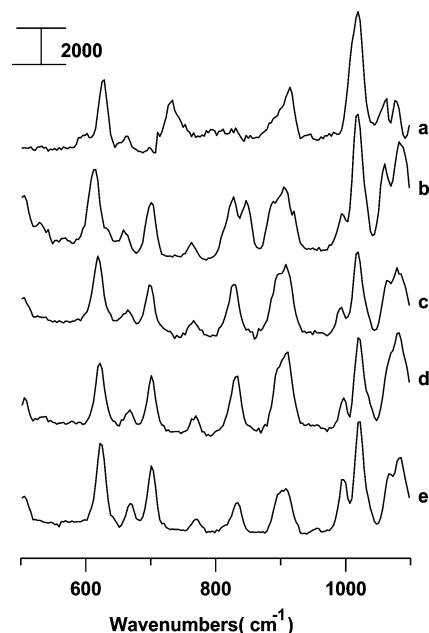


Figure 3. Raman spectra of 1-butyl-3-methylimidazolium chloride obtained under the following pressures: (a) ambient, (b) 0.3, (c) 0.9, (d) 1.5, and (e) 1.9 GPa. The Raman intensity (counts) is labeled on the top left corner.

features showed further evolution through the observation of bandwidth narrowing for the peaks at ca. 830 and 900 cm^{-1} . Analysis of the pressure-dependence shows that the characteristic band at 613 cm^{-1} in Figure 3b was blue-shifted to 619 cm^{-1} in Figure 3c, but the characteristic band at 700 cm^{-1} in Figure 3b was slightly red-shifted to 698 cm^{-1} in Figure 3c. These results suggest that a structural relaxation or a second phase transition is taking place. As the pressure was elevated to 1.5 GPa (Figure 3d), both of the characteristic bands were blue-shifted again to 622 and 701 cm^{-1} , respectively. We note that Figures 3e and 1e are almost identical in spectral features. In other words, the GA form, being a less stable form for 1-butyl-3-methylimidazolium chloride under ambient pressure, is switched to a more stable state under the condition of high-pressure.

We obtained insight into the new high-pressure phase by measuring the pressure-dependent variations in the IR spectra of 1-butyl-3-methylimidazolium bromide in the crystalline form. Figure 4 presents IR spectra of pure 1-butyl-3-methylimidazolium bromide obtained under ambient pressure (curve a) and at 0.3 (curve b), 0.9 (curve c), 1.5 (curve d), and 1.9 GPa (curve e). Table 1 displays the predicted C–H stretching frequencies of the 1-butyl-3-methylimidazolium cation in the AA and GA forms, respectively. Harmonic vibrational frequencies were obtained from analytical second derivatives at the B3LYP/6-31+G* level using the Gaussian 03 program package.²⁷ The scaling factor for the calculated frequencies is 0.955.^{21–24,28} As indicated in Figure 4a, the absorption bands at ca. 3082, 3090, 3104, and 3136 cm^{-1} correspond to coupled imidazolium C–H stretching vibrations with three hydrogen atoms bound to the imidazolium ring. The absorption bands at ca. 2880 and 2967 cm^{-1} are attributed to C–H stretching modes of the methyl and butyl groups. As shown in Figure 4b–e, the compression leads to continuous loss of the 3090 cm^{-1} band intensity. The pressure dependence of the C–H stretches yielded blue frequency shifts in Figure 4. As shown in Figure 4e, the C–H stretches were blue-shifted to 2889, 2981, 3083, 3114, and 3144 cm^{-1} .

Figure 5 displays IR spectra of 1-butyl-3-methylimidazolium chloride in crystalline form obtained under ambient pressure

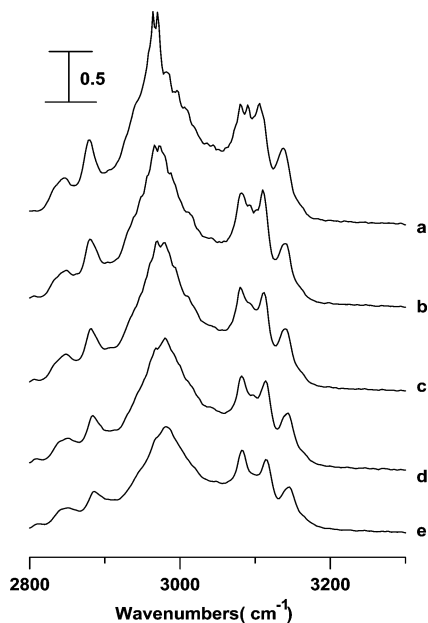
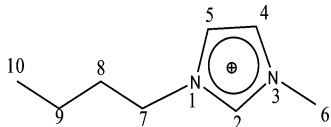


Figure 4. IR spectra displaying the C–H stretching region of pure 1-butyl-3-methylimidazolium bromide under (a) ambient pressure and at (b) 0.3, (c) 0.9, (d) 1.5, and (e) 1.9 GPa.

TABLE 1: DFT-calculated C–H Stretching Frequencies (cm^{-1}) and IR Intensities (km/mol) of 1-Butyl-3-methylimidazolium Cation

calc'd frequencies (AA/GA) ^a	intensities (AA/GA)	assignment ^b
3168/3168	8/7	sym C ^{4,5} –H
3157/3158	27/27	C ² –H
3152/3152	14/14	asym C ^{4,5} –H
3047/3047	0.5/0.5	asym C ⁶ –H (methyl)
3032/3032	0.3/0.3	asym C ⁶ –H (methyl)
3002/3001	9/6	butyl C–H
2987/2986	21/20	butyl C–H
2974/2975	41/37	butyl C–H
2953/2956	12/19	butyl C–H
2953/2953	6/6	sym C ⁶ –H (methyl)
2944/2945	18/7	butyl C–H
2920/2915	2/29	butyl C–H
2913/2911	30/15	butyl C–H
2904/2907	25/13	butyl C–H
2895/2883	9/31	butyl C–H

^a Frequencies scaled by 0.955. ^b Numbering of the skeleton atoms for the 1-butyl-3-methylimidazolium cation



(curve a) and at 0.3 (curve b), 0.9 (curve c), 1.5 (curve d), and 1.9 GPa (curve e). As the Br^- was replaced by Cl^- , compare Figures 4a and 5a, the imidazolium C–H absorption bands were blue-shifted to 3095, 3126, and 3154 cm^{-1} in Figure 5a. It is likely that the hydrogen-bonding patterns are determined by the relative hydrogen-bonding acceptor strength of Br^- and Cl^- . As we know, the vibrational modes undergo a red frequency shift and accompanying intensification upon formation of the conventional hydrogen-bond via $\text{N}^{\text{H}}\cdots\text{O}$ or $\text{O}^{\text{H}}\cdots\text{O}$ interactions. However, in a number of cases, the $\text{C}^{\text{H}}\cdots\text{X}$ and $\text{C}^{\text{H}}\cdots\text{O}$ interactions lead to shortening of the bridging C–H bond, that is, blue-shifting hydrogen-bonding, and not the lengthening that is generally considered a typical feature of a hydrogen-bond.^{18–20} On the basis of the results of Figures 4a

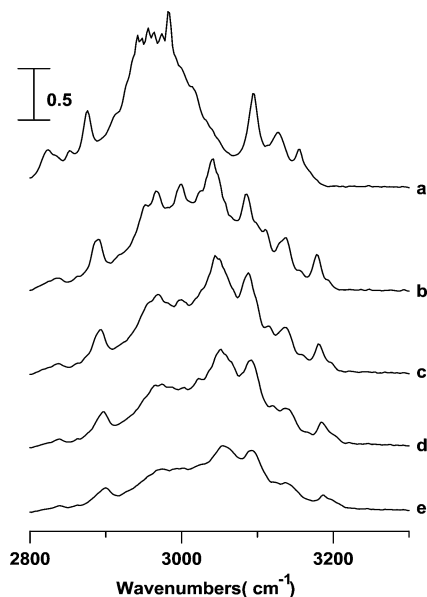


Figure 5. Pressure-dependence of the IR spectra in the C–H stretching region of pure 1-butyl-3-methylimidazolium chloride under the following pressures: (a) ambient, and (b) 0.3, (c) 0.9, (d) 1.5, and (e) 1.9 GPa.

and 5a, we suggest that the Cl^- anion is a stronger blue-shifting hydrogen-bonding acceptor than the Br^- anion. The C–H stretching modes underwent dramatic changes in their spectral profiles as the pressure was elevated to 0.3 GPa in Figure 5b. As revealed in Figure 5a,b, the 3095 cm^{-1} band in Figure 5a was red-shifted to 3085 cm^{-1} in Figure 5b, whereas the absorption frequencies of the 3126 and 3154 cm^{-1} bands in Figure 5a were blue-shifted to 3133 and 3178 cm^{-1} , respectively, in Figure 5b. This fact could be related to the well-known acidity of $\text{C}^2\text{--H}$.²⁹ The anomalous frequency-shifts of imidazolium C–H bands in Figure 5b may be due to the modification of the imidazolium $\text{C}^{\text{H}}\cdots\text{Cl}^-$ contacts upon compression. In the past, consistent models have been proposed for the theoretical understanding of the $\text{C}^{\text{H}}\cdots\text{O}$ and $\text{C}^{\text{H}}\cdots\text{X}$ interactions. For example, when a molecule that is capable of forming blue-shifting hydrogen-bonds binds to a site with a sufficiently strong electrostatic field to dominate over the overlap effect, that molecule is predicted to display a red-shifting hydrogen-bond;²⁰ experimental evidence is still lacking, however. In this article, we present a means of looking at this issue by employing the high-pressure method. In light of this finding, we may be able to attribute the red-shift observed in Figure 5b to strengthening of the imidazolium $\text{C}^2\text{--H}\cdots\text{Cl}^-$ contacts upon compression, that is, a switch to imidazolium $\text{C}^2\text{--H}\cdots\text{Cl}^-$ hydrogen-bond-like. An ab initio study also predicted that the $\text{C}^2\text{--H}\cdots\text{O}$ interactions of aqueous imidazolium are very strong, in the neighborhood of 10 kcal/mol, and should exhibit the features of a strong hydrogen-bond, that is, a red-shifted C–H frequency.³⁰

The alkyl C–H stretching bands separated into four bands at 3039, 2999, 2967, and 2890 cm^{-1} , as shown in Figure 5b. The appearance of the prominent absorption at 3039 cm^{-1} in Figure 5b is interesting, and a subtle balance between the repulsive and attractive force-induced perturbation must be at play. This result may reflect the strengthening of $\text{C}^{\text{H}}\cdots\text{Cl}^-$ interactions between methyl/butyl C–H groups and the Cl^- anion. To rationalize the experimental observations, the alkyl $\text{C}^{\text{H}}\cdots\text{Cl}^-$ hydrogen-bonding is suggested to be a compensatory mechanism to provide stability and to switch the crystal packing from the AA form (Figure 5a) to the GA form (Figure 5b).

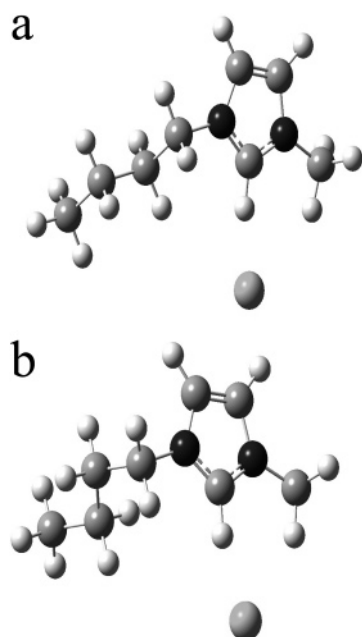


Figure 6. Optimized structures of the 1-butyl-3-methylimidazolium chloride complex in the (a) AA and (b) GA forms.

TABLE 2: Changes in the NBO Charge (methyl) of the Bridging Hydrogen^{a,b}

ΔQ (methyl) ^a		assignment
AA ^b	GA ^c	
20	28	C ² —H
38	64	C ⁶ —H
−1	44	C ⁷ —H
31	17	C ⁸ —
−2	52	C ⁹ —
8	30	C ¹⁰ —

^a Charge changes relative to the monomer ($\Delta Q = Q(\text{complex}) - Q(\text{monomer})$). ^b Structure illustrated in Figure 6a. ^c Structure illustrated in Figure 6b.

Figure 6 displays the optimized density functional theory (DFT)-calculated structure of the 1-butyl-3-methylimidazolium chloride complex with the butyl side in the AA and GA forms, Figure 6a,b, respectively. There is a transfer of net charge that occurs between the cation and the Cl[−] upon formation of hydrogen-bonded complexes. The charge transfer of the 1-butyl-3-methylimidazolium cation was calculated from the natural bond orbital (NBO) charge of Cl[−] and is equal to −159 (methyl) and −156 (methyl) for Figure 6a,b, respectively. The electron density flows from the proton acceptor molecule to the donor, causing a greater negative charge on the latter and a more positive charge on the former. Table 2 indicates electron density loss from the bridging hydrogen atom as the result of C—H...Cl[−] hydrogen-bond formation. As shown in Table 2, the changes in the NBO charges of C⁶—H (methyl), C⁷—H (butyl), C⁹—H (butyl), and C¹⁰—H (butyl) bridging hydrogen in the GA form are more than those in the AA form. This observation may indicate stronger alkyl C—H...Cl[−] interactions in the case of species b in Figure 6. It is known that the bridging proton becomes more positively charged upon formation of the hydrogen-bond. This trend is characteristic of conventional hydrogen-bonds as well as C—H...O hydrogen-bonds.³¹ As revealed in Table 2, the methyl and butyl C—H groups are good proton donor sites for species b in Figure 6. These calculated results are consistent with our pressure-dependent results in Figure 5 that indicate the important role of the alkyl C—H...Cl[−] interactions in switching the crystal packing from the AA

TABLE 3. Relative Energies (hartree/mol) and Total Interaction Energies (kcal/mol)

species ^a	relative energies ^b	interaction energies (− ΔE)
Cl [−]	−460.274 726	
AA monomer	−422.959 537	
GA monomer	−422.958 985	
AA-Cl [−] complex	−883.376 369	89.17
GA-Cl [−] complex	−883.362 814	81.02

^a Structures illustrated in Figure 6. ^b B3LYP/6-31+G* level.

form to the GA form. Energy results revealed in Table 3 were obtained based on the B3LYP/6-31+G* equilibrium geometries. The basic-set superposition error (BSSE) is ca. 0.2 kcal/mol for monomers. As shown in Table 3, the GA-Cl[−] complex (Figure 6b) has a lower total interaction energy than does the AA-Cl[−] complex. In agreement with the theoretical predictions, previous experimental studies^{7,8} observed that 1-butyl-3-methylimidazolium chloride in the AA form is a more stable form at ambient pressure.

It is instructive to note that the calculated results may only provide qualitative support for the suggested C—H...Cl[−] interactions, because the calculations are based on gas-phase structures of the monomer complex. Recently, attention has been paid to the cooperative effect in ionic liquids with increasing cluster size.³² The cooperative effect seems to play a more important role than expected for larger clusters of the dimethylimidazolium cation paired with a chloride anion.³²

Acknowledgment. The authors thank the National Dong Hwa University and the National Science Council (Contract No. NSC 95-2113-M-259-013-MY3) of Taiwan for financial support. The authors thank Ting-Yun Lai for her assistance.

References and Notes

- (1) *Green Industrial Applications of Ionic Liquids*; Rogers, R. D., Seddon, K. R., Volkov, S. Eds.; NATO Science Series; Springer: New York, 2002.
- (2) *Ionic Liquids in Synthesis*; Wasserscheid, P., Welton, T., Eds.; Wiley-VCH: Weinheim, 2002.
- (3) Del Popolo, M. G.; Lynden-Bell, R. M.; Kohanoff, J. *J. Phys. Chem. B* **2005**, *109*, 5895.
- (4) Hardacre, C.; Holbrey, J. D.; McMath, S. E. J.; Bowron, D. T.; Soper, A. K. *J. Chem. Phys.* **2003**, *118*, 273.
- (5) Dupont, J.; Suarez, P. A. Z. *Phys. Chem. Chem. Phys.* **2006**, *8*, 2441.
- (6) Wang, Y.; Li, H.; Han, S. *J. Phys. Chem. B* **2006**, *110*, 24646.
- (7) Holbrey, J. D.; Reichert, W. M.; Nieuwenhuyzen, M.; Johnston, S.; Seddon, K. R.; Rogers, R. D. *Chem. Commun.* **2003**, 1636.
- (8) Ozawa, R.; Hayashi, S.; Saha, S.; Kobayashi, A.; Hamaguchi, H. *Chem. Lett.* **2003**, 32, 948.
- (9) Saha, S.; Hamaguchi, H. *J. Phys. Chem. B* **2006**, *110*, 2777.
- (10) Triolo, A.; Mandanici, A.; Russina, O.; Rodriguez-Mora, V.; Cutroni, M.; Hardacre, C.; Nieuwenhuyzen, M.; Bleif, H.; Keller, L.; Ramos, M. A. *J. Phys. Chem. B* **2006**, *110*, 21357.
- (11) Umebayashi, Y.; Fujimori, T.; Sukizaki, T.; Asada, M.; Fujii, K.; Kanzaki, R.; Ishiguro, S. *J. Phys. Chem. A* **2005**, *109*, 8976.
- (12) Berg, R. W.; Deetlefs, M.; Seddon, K. R.; Shim, I.; Thompson, J. M. *J. Phys. Chem. B* **2005**, *109*, 19018.
- (13) Hunt, P. A.; Gould, I. R. *J. Phys. Chem. A* **2006**, *110*, 2269.
- (14) Lopes, J. N. A. C.; Padua, A. A. H. *J. Phys. Chem. B* **2006**, *110*, 7485.
- (15) Chang, H. C.; Jiang, J. C.; Tsai, W. C.; Chen, G. C.; Lin, S. H. *J. Phys. Chem. B* **2006**, *110*, 3302.
- (16) Chang, H. C.; Jiang, J. C.; Tsai, W. C.; Chen, G. C.; Lin, S. H. *Chem. Phys. Lett.* **2006**, *427*, 310.
- (17) Chang, H. C.; Chang, C. Y.; Su, J. C.; Chu, W. C.; Jiang, J. C.; Lin, S. H. *Int. J. Mol. Sci.* **2006**, *7*, 417.
- (18) Hobza, P.; Havlas, Z. *Chem. Rev.* **2000**, *100*, 4253.
- (19) Gu, Y. L.; Kar, T.; Scheiner, S. *J. Am. Chem. Soc.* **1999**, *121*, 9411.
- (20) Masunov, A.; Dannenberg, J. J.; Contreras, R. H. *J. Phys. Chem. A* **2001**, *105*, 4737.

- (21) Chang, H. C.; Jiang, J. C.; Lai, W. W.; Lin, J. S.; Chen, G. C.; Tsai, W. C.; Lin, S. H. *J. Phys. Chem. B* **2005**, *109*, 23103.
- (22) Chang, H. C.; Jiang, J. C.; Tsai, W. C.; Chen, G. C.; Chang, C. Y.; Lin, S. H. *Chem. Phys. Lett.* **2006**, *432*, 100.
- (23) Lee, K. M.; Chang, H. C.; Jiang, J. C.; Chen, J. C. C.; Kao, H. E.; Lin, S. H.; Lin, I. J. B. *J. Am. Chem. Soc.* **2003**, *125*, 12358.
- (24) Lin, J. S.; Jiang, J. C.; Chang, C. M.; Lai, W. W.; Fang, J. W.; Lin, S. H.; Chang, H. C. *J. Chin. Chem. Soc.* **2005**, *52*, 625.
- (25) Wong, P. T. T.; Moffatt, D. J.; Baudais, F. L. *Appl. Spectrosc.* **1985**, *39*, 733.
- (26) Wong, P. T. T.; Moffatt, D. J. *Appl. Spectrosc.* **1987**, *41*, 1070.
- (27) Frisch, M. J. et al. *Gaussian 03, revision A.7*; Gaussian, Inc.: Pittsburgh, PA, 2003.
- (28) Choi, M. Y.; Miller, R. E. *J. Phys. Chem. A* **2006**, *110*, 9344.
- (29) Eicher, T.; Hauptmann, S. *The Chemistry of Heterocycles*; Stuttgart: New York, 1995.
- (30) Scheiner, S.; Kar, T.; Pattanayak, J. *J. Am. Chem. Soc.* **2002**, *124*, 13257.
- (31) Kar, T.; Scheiner, S. *J. Phys. Chem. A* **2004**, *108*, 9161.
- (32) Kossmann, S.; Thar, J.; Kirchner, B.; Hunt, P. A.; Welton, T. *J. Chem. Phys.* **2006**, *124*, 174506.